SOLID STATE KINETIC PARAMETERS AND MECHANISM FOR THE DEAQUATION–ANATION OF HEXACYANOCOBALTATE(III) OF AQUOPENTAAMMINECOBALT(III), RHODIUM(III) AND IRIDIUM(III), CALCULATED BY ISOTHERMAL DSC MEASUREMENTS

J. RIBAS, A. ESCUER * and M. SERRA

Departament de Química Inorgànica, Facultat de Química, Universitat de Barcelona, Diagonal, 647, 08028 Barcelona (Spain)

(Received 11 November 1985)

ABSTRACT

Three new dinuclear complexes, $[(NH_3)_5M-NC-Co(CN)_5]$, (where M = Co, Rh, Ir) have been obtained by solid state reaction of the corresponding double complexes $[M(NH_3)_5(H_2O)][Co(CN)_6]$. This solid state deaquation–anation has been studied by DSC measurements both in non-isothermal and isothermal conditions. The activation energies so obtained are: 125 kJ mol^{-1} for the Co–Co compound; 87 kJ mol^{-1} for the Rh–Co compound and 104 kJ mol^{-1} for the Ir–Co compound. All these values are in perfect agreement with those previously reported by means of isothermal TG measurements. These low values indicate an SN_1 dissociative mechanism with an activated complex of square-based pyramidal geometry. The low values for the Rh(III) and Ir(III) compounds are explained in terms of the size ratio between cations and anions, which allows the water molecules to escape easily from the crystal lattice in the more voluminous $[M(NH_3)_5(H_2O)][Co(CN)_6]$ (where M = Rh, Ir).

INTRODUCTION

The solid phase thermal reaction of the doubly complexed salt $[M(NH_3)_5(H_2O)][M'(CN)_6]$ (where M, M' = Co, Cr) has been largely studied since Haim and co-workers prepared dinuclear $[(NH_3)_5Co-NC-Co(CN)_5]$ [1,2]. One more systematic study has been recently reported by Uehara and co-workers [3] which discusses the results of the decomposition of nine doubly-complexed salts of this type, under quasi-isothermal and dynamic conditions.

In a very interesting paper, House [4] proposed a general mechanism for solid state dehydration–anation of coordination compounds in which the

---

* Author for correspondence.

generation of a point defect is considered as the formation of the transition state. The dehydration of $[M(NH_3)_5(H_2O)]X_3$ complexes is more consistent, according to House [4] and LeMay and Babich [5] with the formation of a Frenkel type defect and an SN_1 (dissociative) mechanism. In the same field we have found that the dehydration–anation mechanism of several aqua-amine complexes of chromium(III) and cobalt(III) [6] with cyanocomplexes as entering ligands is always consistent with a dissociative mechanism. In this paper, the kinetic parameters are calculated for the deaquation–anation of $[M(NH_3)_5(H_2O)][Co(CN)_6]$ (where $M = Co$, Rh, Ir) and finally the mechanism is discussed, taking into account that for $M = Co(III)$ the kinetics are widely studied [7].

EXPERIMENTAL

Preparation of the starting materials

$[Co(NH_3)_5(H_2O)](ClO_4)_3$ [8], $[Rh(NH_3)_5(H_2O)](ClO_4)_3$ [9], $[Ir(NH_3)_5(H_2O)]ClO_4)_3$ [10] and $K_3[Co(CN)_6]$ [11] were prepared by the same methods as those described in the literature, and they were identified by means of elemental analyses and spectrophotometric measurements.

Preparation of the double complexes

It should be noted that the double complexes obtained were not recrystallized because they are sparingly soluble in water and in the more common solvents; therefore the starting materials for use in the preparation of the double complexes must be fully purified beforehand. A solution of 0.02 mol of $[M(NH_3)_5(H_2O)](ClO_4)_3$ (where $M = Co$, Rh, Ir) in the minimum amount of water is gradually added with continuous stirring to a solution of 0.02 mol of $K_3[Co(CN)_6]$ in the minimum amount of water, passed through an Amberlite cation exchanger resin in the ammonia form. After a few minutes precipitates began to appear. The mixture was then allowed to stand in a

TABLE 1

Analytical data (%) Calcd. (Found)

	C	N	H
$[Co(NH_3)_5(H_2O)][Co(CN)_6]$	19.11 (19.4)	40.87 (41.3)	4.51 (4.3)
$[Rh(NH_3)_5(H_2O)][Co(CN)_6]$	17.11 (17.0)	36.60 (37.1)	4.04 (4.2)
$[Ir(NH_3)_5(H_2O)][Co(CN)_6]$	14.11 (14.4)	30.19 (30.4)	3.33 (3.5)
$[(NH_3)_5Co–NC–Co(CN)_5]$	20.07 (19.8)	42.92 (43.5)	4.18 (4.1)
$[(NH_3)_5Rh–NC–Co(CN)_5]$	17.87 (17.6)	38.23 (38.4)	3.72 (3.9)
$[(NH_3)_5Ir–NC–Co(CN)_5]$	14.63 (14.8)	31.29 (31.4)	3.05 (2.9)

refrigerator overnight to complete its precipitation. The precipitate thus obtained was collected by filtration, washed several times with ice-cold water, ethanol and ether, and air-dried. All the double complexes were obtained in almost quantitative yields. Table 1 summarizes the analytical data for the complexes obtained.

Techniques

Infrared spectra of the samples were measured with a Beckman IR-20-A spectrophotometer, purged with dry-air, by the KBr disk method or Nujol suspension. Calorimetric studies were carried out on a Perkin-Elmer model DSC-2 system in a nitrogen atmosphere with the perforated capsules to permit the elimination of the water produced during the process, the sample size being in the range of 5–7 mg. The heating rate for non-isothermal experiments was $5°C$ min^{-1}.

Kinetic parameters

The kinetic parameters were determined on the basis of the general kinetic relation [12]

$$d\alpha/dt = k(T)f(\alpha)$$

In this work we have used all the principal expressions of $f(\alpha)$ indicated in the literature [12], following the four physical models of solid state chemistry: nucleation, growth, nucleation–growth and diffusion (Table 2). To find the real kinetic parameters we have compared the variable values obtained for non-isothermal measurements with the almost constant values

TABLE 2

Kinetic functions, $g(\alpha)$, used in their integral form

Mechanism	$g(\alpha)$
Nucleation controlled	
Exponential law	$\ln \alpha^n$
Power law	$\alpha^{1/n}$
Growth controlled	$[1-(1-\alpha)^{1-n}]/(1-n)$
for $n=1$	$[-\ln(1-\alpha)]$
Nucleation – growth controlled	
Avrami–Erofeev	$[-\ln(1-\alpha)]^{1/n}$
Prout–Tompkins	$\ln[\alpha/(1-\alpha)]$
Diffusion controlled	
One-dimensional	α^2
Two-dimensional	$\alpha+(1-\alpha)\ln(1-\alpha)$
Three-dimensional	$[1-(1-\alpha)^{1/3}]^2$
Three-dimensional	$(1-2/3\alpha)-(1-\alpha)^{2/3}$

for any model in the isothermal measurements and we have taken into account the best r^2 (regression coefficient) value. In the non-isothermal measurements we employed the approximation of Coats and Redfern [13].

RESULTS

Characterization of the double complexes and dinuclear compounds

All the double complexes are isostructural, and the structures of $[Co(NH_3)_6][Co(CN)_6]$ and $[Co(NH_3)_6][Cr(CN)_6]$ are known [14]. A previous study of this isostructuralism has been reported [15]. Taking into account the importance of this isostructuralism in order to discuss the variation in the kinetic parameters in the Co, Rh, Ir series, it will be very useful to summarize the results here: all the complexes belong to the spatial group R$\bar{3}$, with $Z = 1$; the M and M' atoms are placed on the $\bar{3}$ axis. The structure consists of a pair of $[M(NH_3)_5(H_2O)]^{3+}$ and $[Co(CN)_6]^{3-}$ ions placed in a rhombohedral cell having the CsCl structure type.

The IR spectra of all these complexes show the typical bands of the CN, NH$_3$ and H$_2$O groups. The three more characteristic bands are $\nu(CN)$, $\delta_s(NH_2)$ and $\rho(NH_3)$ (Table 3). The $\delta_s(NH_2)$ is shifted 20–30 cm^{-1} towards higher frequencies in the double salts, compared with the starting perchlorate. The rocking band is also shifted towards higher frequencies, increasing by about 30 cm^{-1} in the Ir(III) compound. These shifts are consistent with the existence of hydrogen bonding between anion and cation, as has been pointed out by Nakamoto [16] and Novak [17], in similar complexes. Such hydrogen bonding has been shown in the [Co(NH$_3$)$_6$][Co-(CN)$_6$] structure [14], with the N $\cdots$ H $\cdots$ N distance 3.000(6) Å.

TABLE 3

Selected bands for IR spectra

	$\nu(CN)$	$\delta(NH_2)$	$\rho(NH_3)$
$[Co(NH_3)_5(H_2O)](ClO_4)_3$	–	1310 (vs)	830 (s)
$[Co(NH_3)_5(H_2O)][Co(CN)_6]$	2130 (vs)	1330 (vs)	840 (s)
$[(NH_3)_5Co-NC-Co(CN)_5]$	2125 (vs) / 2200 (s)	1330 (vs)	855 (s)
$[Rh(NH_3)_5(H_2O)](ClO_4)_3$	–	1335 (vs)	845 (vs)
$[Rh(NH_3)_5(H_2O)][Co(CN)_6]$	2130 (vs)	1355 (vs)	860 (s)
$[(NH_3)_5Rh-NC-Co(CN)_5]$	2130 (vs) / 2210 (s)	1330 (vs)	850 (s)
$[Ir(NH_3)_5(H_2O)](ClO_4)_3$	–	1370 (vs)	850 (s)
$[Ir(NH_3)_5(H_2O)][Co(CN)_6]$	2130 (vs)	1390 (vs)	890 (s)
$[(NH_3)_5Ir-NC-Co(CN)_5]$	2125 (vs) / 2200 (s)	1350 (s)	880 (s)

The more important region for the characterization of these cyano complexes is the ν(CN) stretching region between 2000–2200 cm^{-1} [18]. In the doubly-complexed salts it appears as a very strong and defined band (Table 3), according to the literature data for $[Co(CN)_6]^{3-}$ salts [18]. In the dinuclear complexes with the μ–CN ligand there is a significant difference with respect to the starting double complexes. There appears to be a very intense and perfectly defined doublet at the ν(CN) zone (Table 3). The clear splitting of the CN stretching frequencies is good evidence for a bridging cyano group [19]. According to the literature data the component occurring at a lower frequency is assigned to the ν(CN) of the terminal cyano group, while that appearing at a higher frequency is attributed to the ν(CN) of the bridging cyano group [19].

DSC of the double complexes

The non-isothermal DSC curves for the solid phase thermal deaquation of $[M(NH_3)_5(H_2O)][Co(CN)_6]$ are very similar. The initial and final temperatures together with weight loss in each case are shown in Table 4. In the three cases there is a mass loss corresponding exactly to one mole of water for each mole of product. In these cases, a new compound was obtained at the end of the curve (or at the end of isothermal runs). This new product corresponds to $[(NH_3)_5M-NC-Co(CN)_5]$ (where M = Co, Rh, Ir) according to analysis (Table 1) and IR measurements (Table 3) (see above). After the water loss, the $[Co(NH_3)_5(H_2O)][Co(CN)_6]$ complex immediately begins to decompose. Instead, the Ir run can be prolonged until a temperature of 200–220°C has been reached without significant decomposition. The Rh compound behaves as an intermediate.

In order to test the validity of the DSC isothermal runs, we compared the ΔH for the dynamic DSC and the isothermal at each temperature. The results are given in Table 4.

In Fig. 1 the dynamic TG run and the integrated dynamic DSC run for $[Co(NH_3)_5(H_2O)][Co(CN)_6]$ are given. A small deviation in the reaction

TABLE 4

Initial and final temperatures for the dynamic DSC corresponding to the loss of coordinated water

	t_{in}	t_f	Weight loss equivalent	ΔH [a] (kJ mol^{-1})	$\Delta H_{average}$ [b] (kJ mol^{-1})
$\lvert Co(NH_3)_5(H_2O)\rVert Co(CN)_6\rvert$	155	210	$1H_2O$	54.9	51.9 ± 4
$\lvert Rh(NH_3)_5(H_2O)\rVert Co(CN)_6\rvert$	132.5	187.5	$1H_2O$	76.8	86.2 ± 5
$\lvert Ir(NH_3)_5(H_2O)\rVert Co(CN)_6\rvert$	150	205	$1H_2O$	78.1	85.6 ± 5

[a] Non-isothermal conditions.
[b] Isothermal conditions.
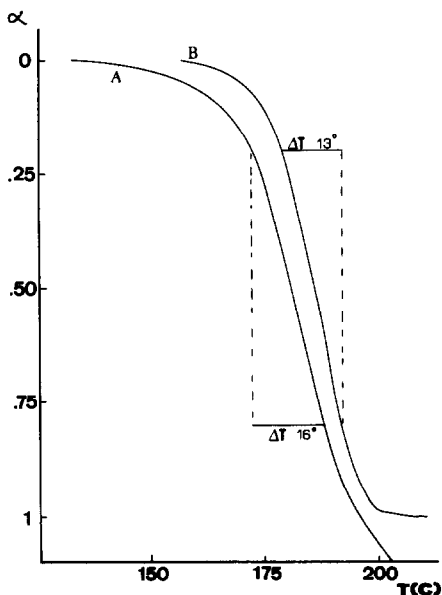
Fig. 1. Dynamic TG run (A) and integrated dynamic DSC (B) run for $[Co(NH_3)_5(H_2O)]$-$[Co(CN)_6]$. The runs for the Rh and Ir analogues are very similar.

temperature can be observed. This deviation may be attributed to the different experimental conditions determined by the shape of the furnace in both techniques. The loss of weight corresponds in the TG exactly to 18 a.m.u. In the DSC the loss of weight is also 18 a.m.u., according to the weight before and after the thermogram.

The most important feature in these thermograms is the difference, ΔT, between the points at which $\alpha = 0.2-0.8$. For $[Co(NH_3)_5(H_2O)][Co(CN)_6]$ this difference is 16°C in the TG run and 13°C in the DSC run. For the Rh(III) and Ir(III) analogues these differences are, respectively 19 and 13°C for Rh(III) and 11 and 11.5°C for Ir(III). Taking into account that $1/\Delta T$ is the most important mathematical factor in the final E_a value, as has been demonstrated [20], a difference of 3–4°C in ΔT respresents a deviation of 20–25% in the E_a value.

Kinetic parameters

Kinetic parameters are very difficult to calculate unambiguously from only non-isothermal curves, due to the fact that the true $g(\alpha)$ expression of the solid state model is not known. For this reason we have recorded not only the non-isothermal curves for each compound but also the isothermal curves at several different temperatures for each compound (Fig. 2). In both methods (non-isothermal and isothermal) all the principal expressions of $g(\alpha)$ reported in the literature [12] have been used. The computation for
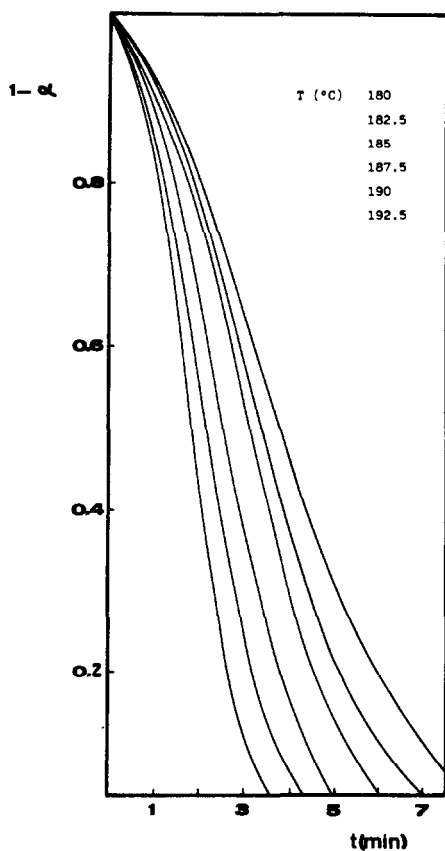
Fig. 2. Integrated isothermal DSC curves (indicating the temperature) for $[Co(NH_3)_5$-$(H_2O)][Co(CN)_6]$. The other two complexes show very similar curves (at 145; 147.5; 150; 152.5; 155; 162.5°C for the Rh complex and 162.5; 165; 167.5; 170; 172.5; 175°C for the Ir complex).

each $g(\alpha)$ and for each n has been carried out with an ad hoc FORTRAN IV program.

The values of E_a and k_0 have been deduced from the isothermal curves since the values so obtained are almost independent of the solid state model proposed [21]. The average kinetic parameters, taking into account the model proposed, are given in Table 5.

TABLE 5

Average kinetic parameters (E_a in kJ mol^{-1}; n for Avrami–Erofeev law)

	E_a	$\ln k_0$	r^2	n
$|Co(NH_3)_5(H_2O)\|Co(CN)_6|$	125.6	31.7	0.9901	2
$|Rh(NH_3)_5(H_2O)\|Co(CN)_6|$	86.9	19.0	0.9970	2.5
$|Ir(NH_3)_5(H_2O)\|Co(CN)_6|$	104.8	23.1	0.9956	2.5

With regard to the physical model (solid-state mechanism) many investigations made so far with non-isothermal methods accept or assume the reaction mechanism, i.e., a specific function $g(\alpha)$ or $f(\alpha)$. In order to avoid assumptions, we consider that the reaction mechanism may be established by comparing the dynamic and isothermal results, as also suggested by other authors [22]. The advantage of this method is the fact that one does not assume the mechanism and the order of the reaction, but all kinetic parameters are determined from experimental results.

In order to choose the appropriate solid-state mechanism it is necessary to take into account two things: (a) the best regression coefficient, r^2 and (b) the shape of the isothermal curves. The Avrami–Erofeev model gives, in all three cases, a best r^2. Furthermore, due to the sigmoid shape of the isothermal curves it is possible that the solid state model corresponds effectively to the nucleation–growth process, according to the Avrami–Erofeev law. The literature [12] indicates that the sigmoid shape agrees with the Avrami–Erofeev law; the greater the sigmoid shape the higher the n value.

DISCUSSION

House [4] has recently proposed several mechanisms in the thermal dehydration–anation reaction of solid complexes, determined by various types of defects: Schottky defects with an SN_2 associative mechanism or Frenkel-type defects with an SN_1 dissociative mechanism. According to this theory, high values of E_a have a better correspondence with an SN_2 mechanism while low values have a better correspondence with an SN_1. Following the crystal field model of Basolo and Pearson [23] the transition state (activated complexes) and the crystal field activation energy (CFAE) values for each metal are given in Table 6 (the Dq values for Co(III), Rh(III) and Ir(III) are those indicated by Huheey [24]). If the mechanism was associative, only the octahedral wedge transition state would give the CFAE values agreeing with the experimental data (the values for the pentagonal bipyramid transition state are too high). However, considering that in the SN_2 reaction the heptacoordination suggests a Schottky-type defect formation in an ionic crystal, it requires high energy ($E_{Sch.} = 0.24\ U$, U being the lattice energy [25]). In our case, the ionic charge is $+3$ and -3; therefore the lattice energy must be very large. Consequently, we should find a value of E_a greater than the values we found (Table 5).

The mechanism, therefore, might be an SN_1 (dissociative) with the formation of a square-based pyramid activated complex. If we suppose a trigonal bipyramid activated complex, it would require a very large CFAE, incompatible with our experimental data. Consequently, the transition state is determined by the water loss and non-ionic Frenkel defect formation.

TABLE 6

Crystal field activation energies for $[M(H_2O)(NH_3)_5]^{3+}$

Mechanism	Intermediate	CFAE	$[CoH_2O(NH_3)_5]^{3+}$ $Dq = 25$ kJ mol^{-1}	$[RhH_2O(NH_3)_5]^{3+}$ $Dq = 38$ kJ mol^{-1}	$[IrH_2O(NH_3)_5]^{3+}$ $Dq = 45$ kJ mol^{-1}
Dissociative	Square-based pyramid	$4Dq$	100	152	180
	Trigonal bipyramid	$11.48Dq$	287	436	516
Associative	Pentagonal bipyramid	$8.52Dq$	213	323	383
	Octahedral wedge	$3.63Dq$	91	138	163

But there is less than perfect agreement between our experimental results and the CFAE theory of Basolo and Pearson. Effectively, according to this theory (Table 6) the CFAE for Ir(III) is 180 kJ mol^{-1}; 152 kJ mol^{-1} for Rh(III) and 100 kJ mol^{-1} for Co(III). Therefore, the E_a for Rh(III) and Ir(III) complexes would be expected to increase by an order of magnitude. The experimental results are different. In the Co(III) case, the E_a value is greater than the contribution of CFAE (100 kJ mol^{-1}), which seems reasonable. But in the Rh(III) and Ir(III) complexes, the E_a values are lower than the expected CFAE contribution (as seen from Tables 5 and 6). Due to the repetition of DSC (and TG) measurements, this factor cannot be attributed to the experimental error, but is due to the compounds. On the other hand, we have found the same anomaly in the isostructural series $[M(NH_3)_5(H_2O)][Cr(CN)_6]$ and $[M(NH_3)_5(H_2O)][CrNO(CN)_5]$, (where M = Co, Rh, Ir) [26].

Why this anomaly? According to the Basolo and Pearson theory there are other unknown factors to add to Dq (these factors can be either positive or negative). House [4], on the other hand, already indicates that even the recent literature persists in trying to describe solid state reactions in terms applicable to processes carried out in the homogeneous phase (gas or solution). This is not correct: it is necessary to take into account the factors derived from the relative size of the ions, the quantification of which has not been possible until now. For a given size of anion, diffusion of interstitial defects depends on the size of the cation or on the comparative size of anion and cation. In fact, interstitial diffusion of Frenkel defects is enhanced by a greater difference in size between ions (the volume of the free space is greater). Thus, if water is set free from the complex ion in forming the transition state, the space of the water molecule will be facilitated for $[Rh(NH_3)_5(H_2O)]^{3+}$ and $[Ir(NH_3)_5(H_2O)]^{3+}$, the largest cations. For this reason, the diffusion of water would be enhanced and the activation energy would be lower than that expected for the CFAE values.

Naturally, this reasoning will be valid only if the known structures are similar (isostructuralism), as is in our case. Consequently, the difference in the free space cannot be attributed to the structural differences but to the relative sizes of the ions.

The importance of this concept of free space has already been studied and reported by us in a series of several complexes such as $[Co(NH_3)_5(H_2O)]_2$-$[M(CN)_4]_3$ (where M = Ni, Pd, Pt)—three isostructural salts in which the E_a value of the Pt compound is lower due to the formation of strong Pt–Pt interactions in the crystal lattice [27]. These interactions allow the molecule of water to escape easily from the crystal. In the series trans-$[CrF(H_2O)(aa)_2][M(CN)_4]$ (where aa = ethylenediamine, 1,3-diaminepropane or 1,2-diaminecyclohexane) we also found that the greater the ligand volume, the lower the activation energy [6].

CONCLUSION

Both the TG and DSC results confirm the reliability of the calculation of the kinetic parameters with isothermal procedures, regardless of the technique, Fig. 3. Instead, with non-isothermal measurements the deviation is very important, derived from the great influence of the ΔT between α 0.2–0.8. Moreover, the results confirm the chemical mechanism (SN_1), but the calculated activation energy is not constant, being lower, in the Rh(III) and Ir(III) cases than that expected, taking into consideration the CFAE theory of Basolo and Pearson. We propose that it is due to the different size ratio between cations and anion, which allows the water molecule to escape easily from the crystal lattice in the more voluminous $[M(NH_3)_5(H_2O)]^{3+}$ (where M = Rh, Ir) cations.

Since there are few studies of solid state reactions of Rh(III) and Ir(III) we hope, in the future, to study this apparent anomaly in other complexes of these cations, with other entering anions to compare with the behaviour of the known Co(III) analogues. It is hoped that such work will determine whether the effect of the relative sizes of the ions and the free space is more important than the Dq contribution of the metal ion.
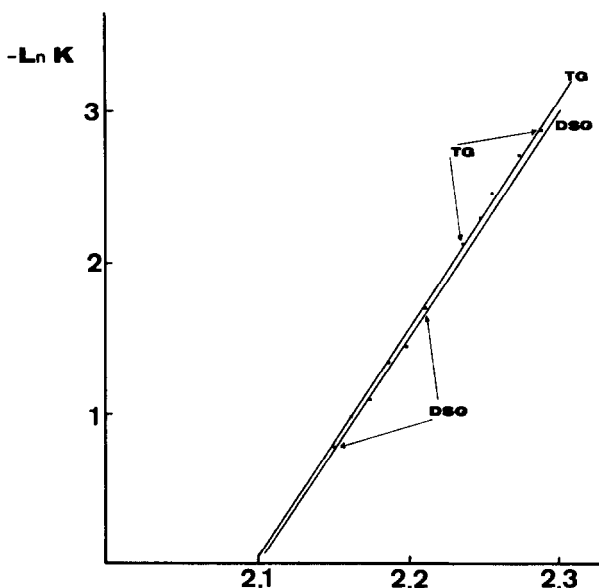

Fig. 3. ln K vs. $1/T$ for isothermal TG and DSC runs in $[Co(NH_3)_5(H_2O)][Co(CN)_6]$, indicating the agreement in both techniques. The figures for Rh and Ir analogues are very similar.

REFERENCES

1 R.A. Castelló, C. Piriz, E. Egen and A. Haim, Inorg. Chem., 8 (1969) 700.
2 C.A. Jepsen and J.E. House, J. Inorg. Nucl. Chem., 43 (1981) 953.
3 A. Uehara, S. Terabe and R. Tsuchiya, Inorg. Chem., 22 (1983) 2864.
4 J.E. House, Jr., Thermochim. Acta, 38 (1980) 59.
5 H.E. LeMay and M.W. Babich, Thermochim. Acta, 48 (1981) 147.
6 J. Ribas, A. Escuer, M. Serra and M.D. Baró, Thermochim. Acta, 56 (1982) 183; M. Serra, A. Escuer and J. Ribas, Thermochim. Acta, 64 (1983) 237; M. Monfort, M. Serra, A. Escuer and J. Ribas, Thermochim. Acta, 69 (1983) 397; M. Corbella, C. Diaz, A. Escuer, A. Seguí and J. Ribas, Thermochim. Acta, 74 (1984) 23.
7 J.E. House, Jr, and B.J. Smith, J. Inorg. Nucl. Chem., 39 (1977) 777; E.L. Simmons and W.W. Wendlandt, J. Inorg. Nucl. Chem., 33 (1971) 3588; C.A. Jepsen and J.E. House, J. Inorg. Nucl. Chem., 43 (1981) 953.
8 G. Schlessinger, Inorganic Laboratory Preparations, Chemical Publishing Company, New York, 1962, p. 206.
9 J.A. Osborn, K. Thomas and G. Wilkinson, Inorg. Synth., 13 (1970) 213; T.W. Swaddle, and R.D. Stranks, J. Am. Chem. Soc., 94 (1972) 8357.
10 H.H. Schnidte, Inorg. Synth., 2 (1946) 243.
11 J.H. Bigelow, Inorg. Synth., 2 (1946) 203.
12 M.E. Brown, D. Dollimore and A.K. Galwey, in Comprehensive Chemical Kinetics, Vol. 22, Elsevier, Amsterdam, 1980, Ch. 3.
13 A.W. Coats, and J.D. Redfern, Nature (London), 201 (1964) 68.
14 M. Iwata and Y. Saito, Acta Crystallogr. B, 29 (1973) 822; M. Iwata, Acta Crystallogr. Sect. B, 33 (1977) 59.
15 J. Ribas, M. Monfort and X. Solans, An. Quim., 80 (1984) 288.
16 K. Nakamoto, Infrared and Raman Spectra of Inorganic and Coordination Compounds, 3rd edn., Wiley, New York, 1978, p. 197.
17 A. Novak, J. Chem. Phys., 72 (1975) 981.
18 A.G. Sharpe, The Chemistry of Cyano Complexes of the Transition Metals, Academic Press, London, 1976, p. 232.
19 D.A. Dows, A. Haim and W.W. Wilmarth, J. Inorg. Nucl. Chem., 21 (1961) 33; J. Casabó, J. Ribas, J.M. Coronas and M. Serra, Inorg. Chim. Acta, 36 (1979) 41; J. Ribas, M. Serra and A. Escuer, J. Inorg. Nucl. Chem., 43 (1981) 3113.
20 A. Escuer, Thesis, Universidad Barcelona, 1984.
21 J.M. Criado, M. Gonzalez, A. Ortega and C. Real, J. Therm. Anal., 29 (1984) 243.
22 J. Zsako, J. Therm Anal., 5 (1973) 239; D. Blecic and Z.D. Zivkovic, Thermochim. Acta, 60 (1983) 68; A.A. Norris, M.I. Pope and M. Selwood, Thermochim. Acta, 41 (1980) 357; T.B. Tang and M.N. Chandri, J. Therm. Anal., 18 (1980) 247.
23 F. Basolo and R.G. Pearson, Mechanism of Inorganic Reactions, 2nd edn., Wiley, New York, 1967, Ch. 3.
24 J.E. Huheey, Inorganic Chemistry, Harper Row, London 1975, p. 309.
25 H. Schmalzried, Solid State Reactions, Verlag-Chemie, New York, 1974, p. 23.
26 J. Ribas, A. Escuer and M. Monfort, Inorg. Chem., 24 (1985) 1874.
27 J. Ribas, M. Serra and A. Escuer, Inorg. Chem., 23 (1984) 2236.